ELSEVIER

Thermochimica Acta 269/270 (1995) 1–25

thermochimica acta

Isothermal kinetic analysis of solid-state reactions using plots of rate against derivative function of the rate equation ☆

Andrew K. Galwey [a], Michael E. Brown [b]*

[a] *School of Chemistry, Queen's University, Belfast BT9 5AG, Northern Ireland, UK*
[b] *Chemistry Department, Rhodes University, Grahamstown, 6140, South Africa*

Received 16 September 1994; accepted 16 November 1994

Abstract

Since the advent of digital data capture and the development of quick and accurate numerical methods for data processing, the use of rate measurements ($d\alpha/dt$) for kinetic analysis of solid-state reactions has gained in popularity. Rate measurements may readily be obtained through use of isothermal derivative thermogravimetry (DTG), or from isothermal differential scanning calorimetry (DSC) (on the assumption that the evolution or absorption of heat may be used to measure the extent of reaction, α). In this paper, the feasibility and desirability of using plots of experimental $d\alpha/dt$ values against the derivative functions for the various models for solid-state reactions is considered critically and discussed quantitatively.

Keywords: Derivative; Isothermal; Kinetics; Rates

1. Introduction

Kinetic measurements are perhaps most frequently undertaken to obtain information concerning the mechanism of a specified reaction. Such investigations may include the characterisation of reaction stoichiometry, particularly product compositions where mixtures are formed and the identification of intermediates. This information can be of value in contributing towards the theoretical development of the subject generally, by identifying the factors that control reactivity and by understanding the

* Corresponding author.

☆ Presented at the 6th European Symposium on Thermal Analysis and Calorimetry, Grado, Italy, 11–16 September 1994.

SSDI 0040-6031(95)02360-7

significance of participating steps. Empirical measurements of reaction rates may also be of value in the development of industrial processes where the principal objective may be to establish the most effective and efficient conditions that can be exploited in production so that costs, waste and pollution are minimised.

The kinetic equations used to express quantitatively the systematic variations in the extent of chemical change with time during many solid-state reactions are formulated through consideration of the changing geometry of an advancing reactant/product interface. This is the active zone within which the chemical changes occur. The theory of the formulation of these rate equations has been given in the literature [1–5]. These kinetic equations are frequently and conveniently expressed in the form, $g(\alpha) = k(t - t_0)$ (see Table 1), where α is the fractional extent of reaction. Most experimental techniques provide direct measurements of α, e.g. measurements of loss of mass with time during decomposition as in isothermal thermogravimetry (TG). Such isothermal TG data can of course be differentiated with respect to time to give derivative TG (DTG) curves which are directly related to rate ($v = d\alpha/dt$)–time curves. Other techniques such as isothermal differential scanning calorimetry (DSC), produce a record of the rate of heat evolution or absorption (dq/dt) with time which again can be related to the curve of $d\alpha/dt$ against time if the mechanism of reaction does not change with time. Ideally, both isothermal DSC and DTG results, recorded under closely similar conditions, should be compared to confirm the kinetic behaviour. Improvements in instrumental techniques now permit the collection of sufficiently accurate data for kinetic analyses to be based on rate/time or rate/α measurements with the advantages of improved discrimination.

In this article, we are specifically concerned with identifying methods for deciding which of the available rate equations describes, with greatest precision, a set of measured α-time values. If the experimental data fit a rate expression accurately, then the reaction may proceed by the geometric model assumed in the derivation of that expression. Thus, in solid-state kinetic analysis the conclusions are used to identify spatial development of the reaction interface, in contrast with homogeneous kinetic observations which give the reaction order (based on concentration terms) and possibly enable the molecularity to be determined.

Criteria for the excellence of kinetic fits reported in research publications are not always specified and, in practice, identification of the preferred rate equation may be a personal decision by the research workers concerned based on undisclosed reasons. A discussion of distinguishability of rate equations has been given [6]. The present paper further develops and extends aspects of the same problem leading to improved interpretation of the more accurate yield/time data now available from experiment.

Most of the rate equations applied to solid-state reactions are based on theory that was developed from microscopic observations [7] of patterns of interface development, usually through the generation [8] and subsequent growth [9] of nuclei.

The participation of melting, which may be local and/or temporary, is an important possibility in the thermal reactions of many initially solid reactants. The detailed kinetic characteristics in reaction systems of this type have not yet been investigated. The unambiguous demonstration of the occurrence or of the absence of melting during a reaction is not always easily achieved [10].

The decomposition of solids are often studied using rising temperature measurements (TG, DTA, DSC). Kinetic analyses of (fractional reaction α, time, temperature) data enable (in principle) the rate equation ($g(\alpha) = kt$), the activation energy E and the pre-exponential term A to be determined [4], sometimes even from a single experiment, for each reactant. Various different mathematical approaches have been used in the calculation of these parameters [4], although the applications of the different calculations do not always lead to the same rate functions ($g(\alpha) = kt$), or magnitudes of A and E [9]. We have decided to confine our coverage to isothermal kinetics only, because this treatment requires fewer assumptions and results appear to be more consistent and reliable. The points made, however, may also be applicable to non-isothermal kinetic measurements.

2. Testing a kinetic fit

Before deciding which rate expression [4,6] most accurately describes a set of measured α–time values, the following aspects of the kinetic analysis must be addressed.

2.1. α-Range of fit

There is always the possibility of deviation of experimental data from theoretical values at the extremities of reaction. Special consideration should be given to the influence of limiting data (at both low and high α values) on the calculation of the regression line and criteria used to measure excellence of fit. At low α, a separate initial rate process may contribute to product yields. This could result from decomposition of an impurity in the reactant, or from the processes that culminate in the appearance of growth nuclei [9]. When recognised and characterised, this contribution to the product yield–time curve can be subtracted out and the kinetic analysis focused on the dominant reaction alone. Unless recognised and separated, the initial deviation may result in a less precise kinetic fit.

Deviations at high α are usually less easily identified. An unusually slow completion of reaction may be due to a very slow contribution from a later and different rate process, for example the onset of product breakdown or a chemical change of an impurity. Incorrect measurement of the yield corresponding to completion of the specific reaction of interest introduces uncertainty into kinetic analyses. It was shown [11] in studies of dehydration of $Li_2SO_4 \cdot H_2O$ that a 10% variation in the final measured yield of water vapor changed the apparent kinetic behaviour from contracting-volume [4] to first-order.

If various calculated $g(\alpha)$ values for a given reaction are plotted against time, the intercept corresponds to the induction period (including reactant warm-up time, slow initial nucleation, etc.). If, however, early α values include a contribution from an initial reaction, completed at α_i, a plot of $g(\alpha' + \alpha_i)$ (where α' refers to the dominant rate process) against time may not intercept the time axis on completion of the 'true' induction period. Distortion will be greatest at low α' values ($\alpha' \approx \alpha_i$).

2.2. Reactant particle shapes and sizes

Kinetic behaviour is often sensitive both to shapes and absolute sizes of particles and to the relative size distributions. In some reactions of powders it has been shown [12] that nucleus growth can extend beyond the crystallite in which reaction has started, the active interface crossing interparticulate contacts. However, in comparing reaction kinetics between individual single crystals from the same preparation, α–time relationships may be sensitive to the shape of each particular crystal studied [11]. When the three edge-dimensions of a rectangular crystal are approximately equal, the rate expression is close to the contracting-cube equation. For crystals that are more asymmetric, the fit is closer to the contracting-area expression. This aspect of kinetic behaviour is discussed by Delmon [3].

2.3. Variation of kinetic characteristics with temperature

Any change in the reaction mechanism, or the factors controlling reaction rate, is expected to influence overall kinetic behaviour. For example, activation energies for nucleation and for growth steps may be different and thus it must follow that the precise shape of the α–time curve will vary with temperature. A different, but important, influence of temperature appears in reversible dissociations where the contribution from the reverse process increases with the prevailing pressure of product gas, but this effect decreases with increasing reactant temperature [13]. The influence of water vapour on dehydration kinetics can be complicated [14].

2.4. Ambiguities in geometric interpretation

The recognition of the best, or, perhaps more realistically, an acceptable kinetic fit does not necessarily mean that the reaction geometry has been fully characterised. Interpretation of the significance of the rate equation must include the consideration of the possibility that alternative reaction models may operate (see, for example, Ref. [4], p. 84, where several distinct patterns of geometric behaviour give a zero-order reaction). Here, as in other aspects of solid-state chemistry, microscopic observations can provide information that is essential for the formulation of reaction mechanisms.

3. Methods of testing kinetic fit (see Ref. [4], p. 77)

Methods of testing kinetic fit can be classified as follows:

1. Methods requiring measurements of α and t.
2. Methods requiring measurements of $d\alpha/dt$ and t.
3. Methods requiring measurements of $d\alpha/dt$, α and t.

3.1. Methods requiring measurements of α and t

3.1.1. Linearity of plots of g (α) against time

The linearity of plots of calculated $g(\alpha)$ values against time is often used to identify the kinetic expression which most satisfactorily represents the reaction. This can include consideration of fractional values of the exponents, for example in the Avrami-Erofe'ev equation, (A*n*, Table 1) [4, 15]. There are no agreed criteria for the recognition of the 'best fit' (for example: range of α applicable, statistical measurements of deviation, behaviour at limits, etc.). The slopes of these plots give the rate constants.

For reactions in which experimental α–time data points show systematic variations from fit to a particular rate equation, this pattern of deviation may be used to identify a more satisfactory kinetic relationship. This was discussed in our earlier article [6] and will not be further considered here.

3.1.2. Comparisons of the shapes of plots of α against reduced-time

Plots of sets of measured α values for different reactions against reduced-time, i.e. a time scale based on a single central scaling point, such as $\alpha = 0.50$ when $t_r = 1.00$ [16], so that $t_r = t/t_{0.50}$, enable the shapes of curves to be compared with each other and with theoretical expectation for appropriate rate equations [17]. This method is especially useful for the identification of an influence of temperature on curve shape.

3.2. Methods requiring measurements of $d\alpha/dt$ and t

3.2.1. Comparisons of curves of ($d\alpha/dt$) against time with master plots

This approach [18, 19] permits discrimination between alternative rate equations without the requirement of measuring α. Both the rates and the times may be scaled to give plots of reduced-rate against reduced-time (RRRT) [20].

3.3. Methods requiring measurements of $d\alpha/dt$, α and t

3.3.1. Comparisons of curves of ($d\alpha/dt$) against α with master plots

The comparison of shapes of plots of ($d\alpha/dt$) against α with master curves has been recommended by Delmon [3]. Only the first-order rate equation, F1 in Table 1, gives a linear relationship. (A zero-order equation would give a horizontal plot.)

3.3.2. Plots of ($d\alpha/dt$) against the derivative function $f(\alpha)$ (Table 1)

The present paper investigates this method of kinetic analysis. This approach could only be considered worthy of recommendation if it could provide improved distinguishability of measured data (sets of α, $d\alpha/dt$ and t values) between the possible rate equations listed in Table 1. The functions $f(\alpha)$ are obtained from the relationship

$$f(\alpha) = \int (1/f(\alpha))\, d\alpha = kt$$

or

$$d\alpha/dt = k f(\alpha) \qquad (1)$$

Where the yield–time data are accurately represented by a particular function $f(\alpha)$, a plot of the experimental $d\alpha/dt$ values against the values of $f(\alpha)$ calculated for each corresponding value of α will be linear, with slope k (the rate coefficient).

Alternatively, values of $(d\alpha/dt)/f(\alpha)$ will be constant when plotted against either time of α.

This method of kinetic analysis assumes that a given set of $d\alpha/dt$ data can be best described by a function $f_1(\alpha)$ and a rate coefficient k_1. If, however, an incorrect expression, $f_2(\alpha)$, has been selected, the plot is that of $k_1 f_1(\alpha)$ against $f_2(\alpha)$. If both functions are of the form $(1-\alpha)^n$, then when α is small distinguishability will be poor. At higher values of α, k_1 appears to be dependent upon $(1-\alpha)^{(n_1-n_2)}$. In more general terms, several of the functions in Table 1 can be described [21] in terms of expressions of the form $\alpha^p(1-\alpha)^q$ with various values of p and q, so that k_1 could be dependent upon

Table 1
Integral and derivative functions for models used in solid state kinetics

Model	$g(\alpha)=kt$	k_{ref} ($\alpha=0.98$ at $t=100$)	$\alpha=g(t)$
An	$[-\ln(1-\alpha)]^{1/n}$	A2 = 0.01978 A3 = 0.01576 A4 = 0.01406	$-\exp(-(kt)^n)$
B1	$\ln(\alpha/(1-\alpha))$	0.03892	$1/(1+\exp(-kt))$
F1	$-\ln(1-\alpha)$	0.03912	$1-\exp(-kt)$
F2	$(1-\alpha)^{-1}-1$	0.50000	$1-(1/(kt+1))$
Fn	$(1/(n-1)\{(1-\alpha)^{(1-n)}-1\}$		$1-\{1/((n-1)kt+1)\}^{(1/(n-1))}$
R2	$1-(1-\alpha)^{1/2}$	0.008586	$1-(1-kt)^2$
R3	$1-(1-\alpha)^{1/3}$	0.007286	$1-(1-kt)^3$
D1	α^2	0.009604	$(kt)^{1/2}$
D2	$(1-\alpha)\ln(1-\alpha)+\alpha$	0.009018	(Reverse calc.)[a]
D3	$[1-(1-\alpha)^{1/3}]^2$	0.005308	$1-(1-(kt)^{1/2})^3$
D4	$1-2\alpha/3-(1-\alpha)^{2/3}$	0.002730	(Reverse calc)[a]

Model	$v/k=(1/k)(d\alpha/dt)=f(\alpha)$	$v=f(t)$
An	$n(1-\alpha)(-\ln(1-\alpha))^{(n-1)/n}$	$nk^n t^{n-1}\exp(-(kt)^n)$
B1	$\alpha(1-\alpha)$	$k\exp(-kt)(1-\exp(-kt))^{-2}$
F1	$(1-\alpha)$	$k\exp(-kt)$
F2	$(1-\alpha)^2$	$(kt)^{-2}$
R2	$2(1-\alpha)^{1/2}$	$2k(1-kt)$
R3	$3(1-\alpha)^{2/3}$	$3k(1-kt)^2$
D1	$1/2\alpha$	$^{1/2}(k/t)^{1/2}$
D2	$(-\ln(1-\alpha))^{-1}$	(Reverse calc.)[a]
D3	$3(1-\alpha)^{2/3}/[2(1-(1-\alpha)^{1/3})]$	$3[(k/t)^{1/2}(1-(kt)^{1/2})^2/2$
D4	$3/[2((1-\alpha)^{-1/3}-1)]$	(Reverse calc.)[a]

[a] Calculated values of time at set values of α.

$\alpha^{(p_1-p_2)}(1-\alpha)^{(q_1-q_2)}$ or an even more complex function. Another way of stating this is that if $f_2(\alpha)$ can be written as $f_1(\alpha)f_3(\alpha)$, then k_1 will be a function of $f_3(\alpha)$, which may be recognisable by its characteristic shape. This characteristic deviation from linearity, through the systematic comparisons shown below, may be used to identify the most closely applicable kinetic equation.

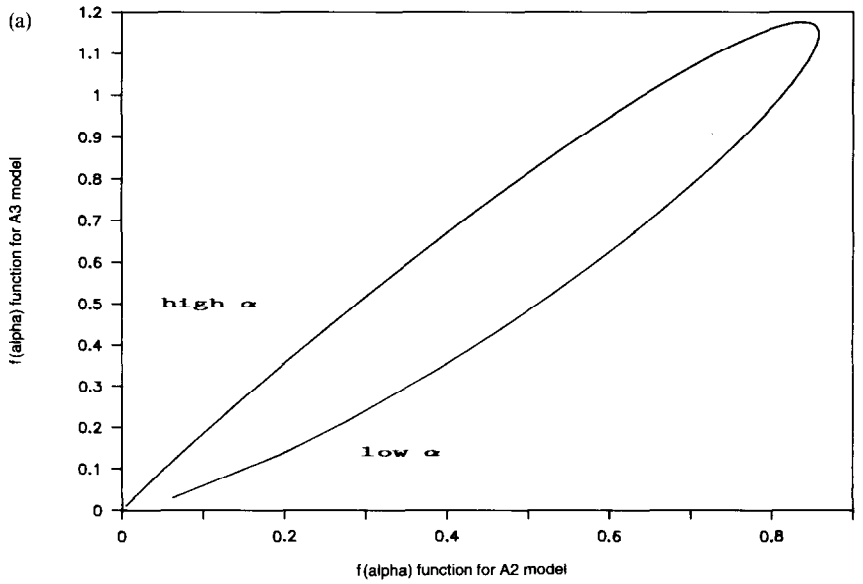

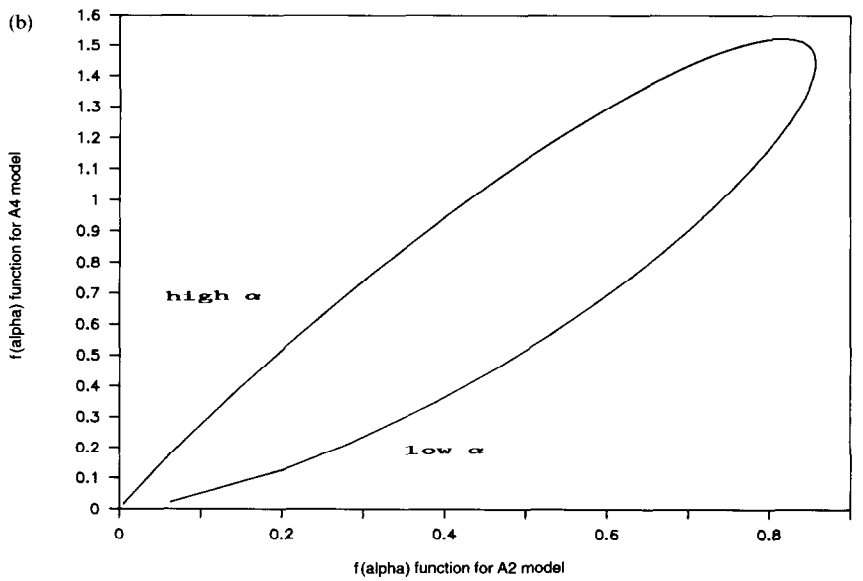

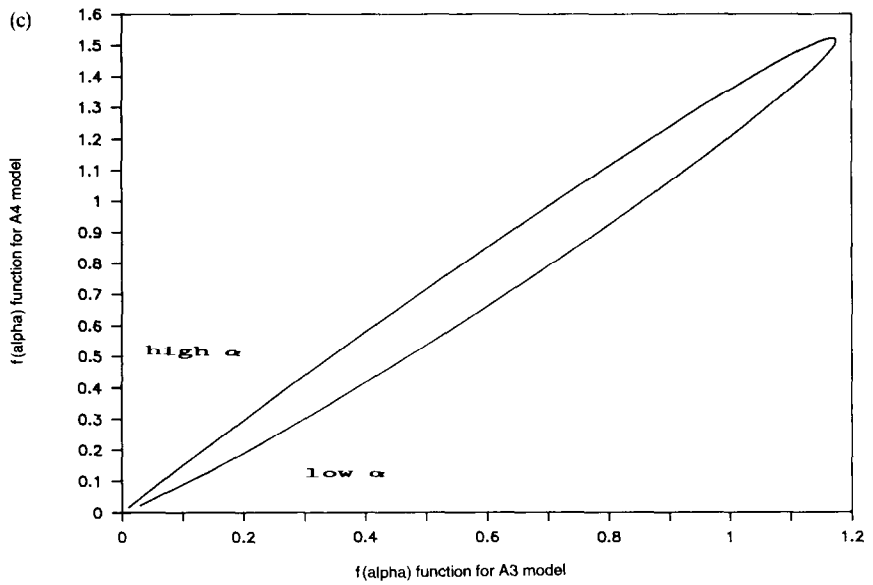

Fig. 1. Rate–rate plots:
(a) $f(\alpha)$ function of A3 model against $f(\alpha)$ function of A2 model;
(b) $f(\alpha)$ function of A4 model against $f(\alpha)$ function of A2 model;
(c) $f(\alpha)$ function of A4 model against $f(\alpha)$ function of A3 model.

It is convenient to consider types of kinetic behaviour in three groups, based on the overall shape of the α–time curve: sigmoid, deceleratory (geometric control) and deceleratory (geometric and diffusion controls).

4. Results and discussion of theoretical kinetic analysis

4.1. *Sigmoid α–time curves*

This set of equations (An, Table 1) has been associated with the names Avrami, Erofe'ev, Johnson, Kohlmogorov, Mampel and Mehl

$$f(\alpha) = v/k = n(1-\alpha)(-\ln(1-\alpha))^{(n-1)/n}$$

Our present analysis has been concerned with values of $n = 2, 3$ and 4, which are those most frequently encountered in reactions of solids [4]; $n = 1$ is the first-order equation (F1). The approach is also readily extended to fractional or higher values of n.

The Prout–Tompkins model (B1) can be expressed as:

$$f(\alpha) = v/k = \alpha(1-\alpha)$$

Autocatalytic behaviour cannot apply from $\alpha = 0$ [22, 23] and the rate equation must incorporate an additional term (or terms). For example

$$v = k_1(1-\alpha)^n + k_2\alpha(1-\alpha)$$

with $k_2 \gg k_1$.

In Fig. 1, $f(\alpha)$ values for the three main An models (A2, A3 and A4, Table 1) are plotted against each other in pairs. The graphs shown identify the form of the deviation when an incorrect rate expression has been selected. A correct kinetic fit will appear as a linear array of points on this derivative plot or, more realistically, including some random scatter, determined by the accuracy of the measurements, about a straight line. The curves have characteristic loops arising from the systematically different shapes of the acceleratory and deceleratory rates for the different values of α. This mismatch is greatest for the A4/A2 comparison and least for the A4/A3 pair, but is clearly apparent in all of the combinations.

In Fig. 2, $f(\alpha)$ values for the models A2, A3 and A4 are plotted against $f(\alpha)$ for the B1 model. The A2/B1 models are the most easily distinguished. The approximate linearity and the decreased separation of the rising and decreasing arms of the loop for the A3/B1 combination indicate the difficulty of distinguishing these models [6]. The A4/B1 combination is slightly more distinguishable. It is of interest that the high α and low α arms of the loops interchange from the A3/B1 combination (Fig. 2(b)) to the A4/B1 combination (Fig. 2(c)).

In Fig. 3, the ratios of $f(\alpha)$ values for combinations of pairs of the models B1, A2, A3 and A4 are plotted against α. Identification of the correct model under these idealised conditions would result in a horizontal line at an ordinate value of 1.00. In real analyses, the ordinate value would be the rate coefficient, k_1, at that isothermal temperature. Fig. 3(a) shows the very characteristic shapes for "incorrect" combinations of the data for the B1 model with the An models, with the symmetry changing with the value of n. Fig. 3(b) shows the very different patterns for selection of the wrong value of n in the combinations of An models. The importance of obtaining accurate values for α during the initial and final stages of reactions which yield sigmoid curves is apparent. It is also evident from the ordinates that a large distortion of the numerical value of k_1 occurs on use of even the closest "incorrect" model. This distortion should not greatly affect the value of the activation energy determined, but will affect the value of the pre-exponential factor A.

4.2. *Deceleratory geometric kinetic models*

The first-order rate equation, F1

$$f(\alpha) = v/k = (1-\alpha)$$

has found frequent application to solid-state reactions. It is of particular interest here because of the difficulty in distinguishing it [6] from the contracting-volume, R3 [11]

$$f(\alpha) = v/k = 3(1-\alpha)^{1/3}$$

and the contracting-area, R2, equations

$$f(\alpha) = v/k = 2(1-\alpha)^{1/2}$$

Occasionally a second-order rate equation, F2 (Table 1)

$$f(\alpha) = v/k = (1-\alpha)^2$$

has found use in heterogeneous kinetics [24], particularly for reactions involving melts or non-crystalline polymers, where conditions may approach those applying during homogeneous reactions in solution.

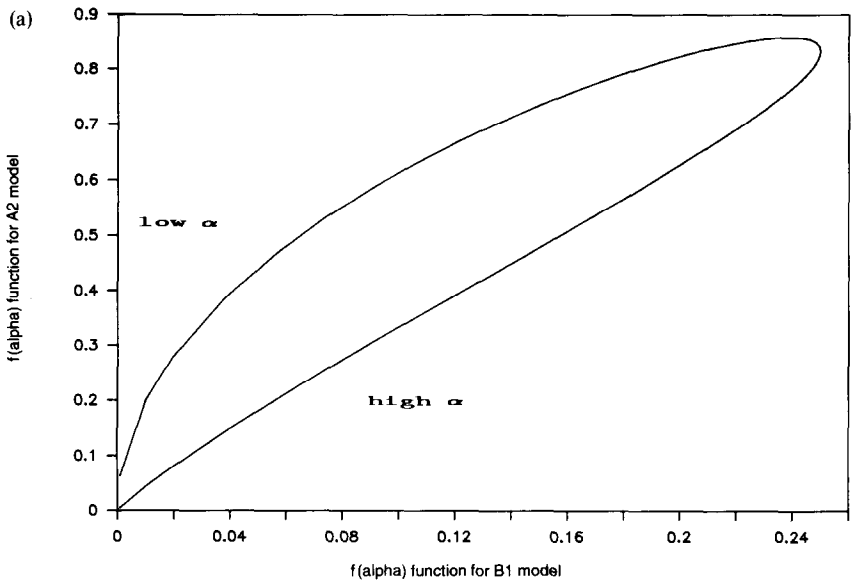

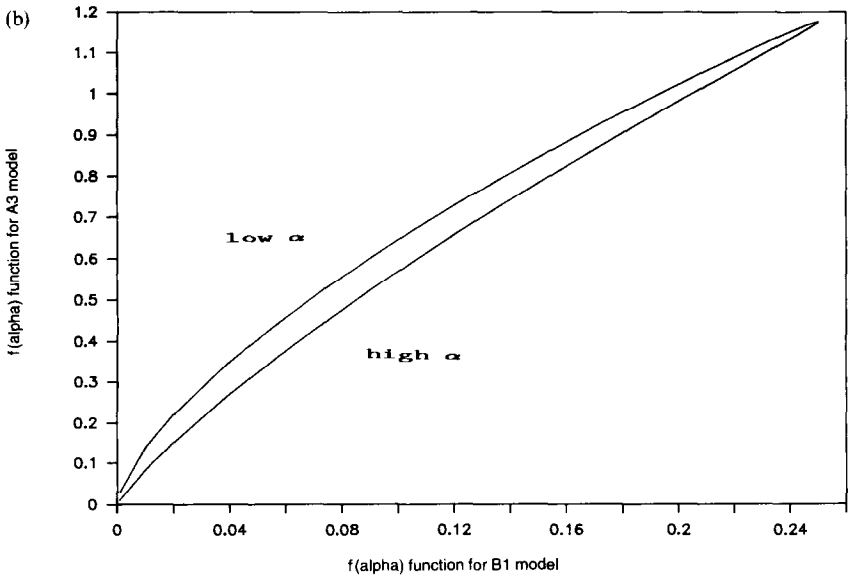

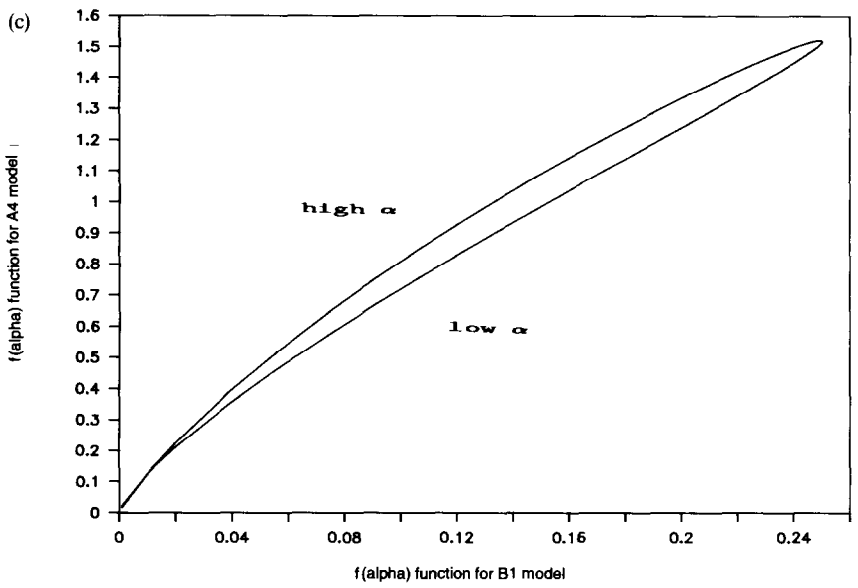

Fig. 2. Rate–rate plots:
(a) $f(\alpha)$ function of A2 model against $f(\alpha)$ function of B1 model;
(b) $f(\alpha)$ function of A3 model against $f(\alpha)$ function of B1 model;
(c) $f(\alpha)$ function of A4 model against $f(\alpha)$ function of B1 model.

In Fig. 4, $f(\alpha)$ values for the rate equations R2, R3, F1 and F2 are plotted against each other in pairs. At low α values, all of the $f(\alpha)$ expressions in this group give plots which are approximately linear and distinguishability is poor. The combination R3/R2 is the most difficult to distinguish [6]. In the graphs in Fig. 4, the regions near the origin, corresponding to high values of α and low reaction rates, show the greatest deviation from linearity. This α range is most important in the kinetic analysis and confirms the need [11] to obtain accurate values of the measured yield corresponding to completion of the reaction being studied. Previous work [11] showed that a 10% change (diminution) in the final product gas pressure used in the calculation of α, changed the apparent kinetic fit from that of the first-order equation to the contracting-volume equation. The first-order expression predicts completion of reaction only after infinite time, whereas the contracting-volume expression results in cessation of reaction when the reaction interface reaches the crystallite centre. Kinetic behaviour is, therefore, most sensitive to characterization of the correct rate equation during the final stages of the rate process.

The above conclusions are demonstrated even more clearly in Fig. 5, where the ratios of $f(\alpha)$ values for combinations of pairs of the R2, R3 and F1 models are plotted against α. The deviations from constancy over the full range of α, increasing further at high α, are apparent.

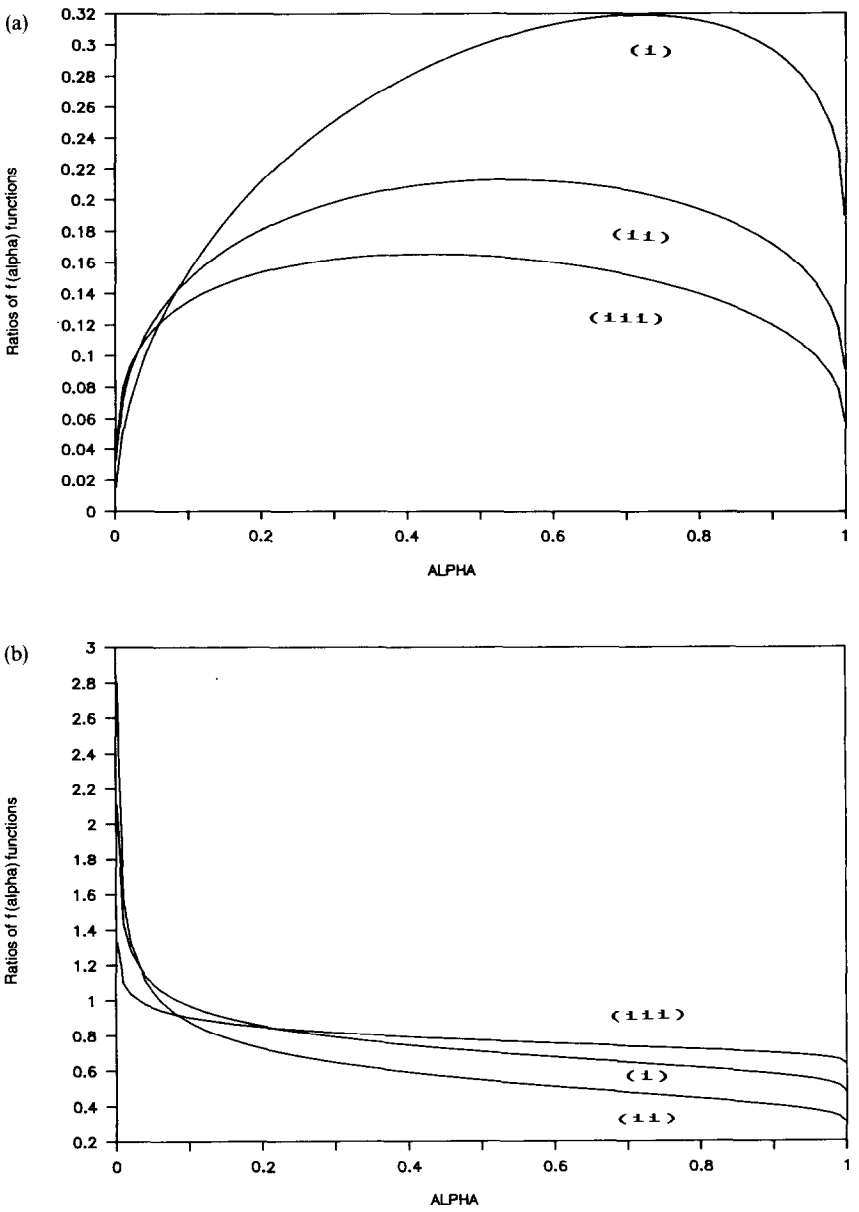

Fig. 3. Ratios of $f(\alpha)$ plots against α:
(a) (i) ($f(\alpha)$ function of B1 model/$f(\alpha)$ function of A2 model) against α;
(ii) ($f(\alpha)$ function of B1 model/$f(\alpha)$ function of A3 model) against α;
(iii) ($f(\alpha)$ function of B1 model/$f(\alpha)$ function of A4 model) against α.
(b) (i) ($f(\alpha)$ function of A2 model/$f(\alpha)$ function of A3 model) against α;
(ii) ($f(\alpha)$ function of A2 model/$f(\alpha)$ function of A4 model) against α;
(iii) ($f(\alpha)$ function of A3 model/$f(\alpha)$ function of A4 model) against α;

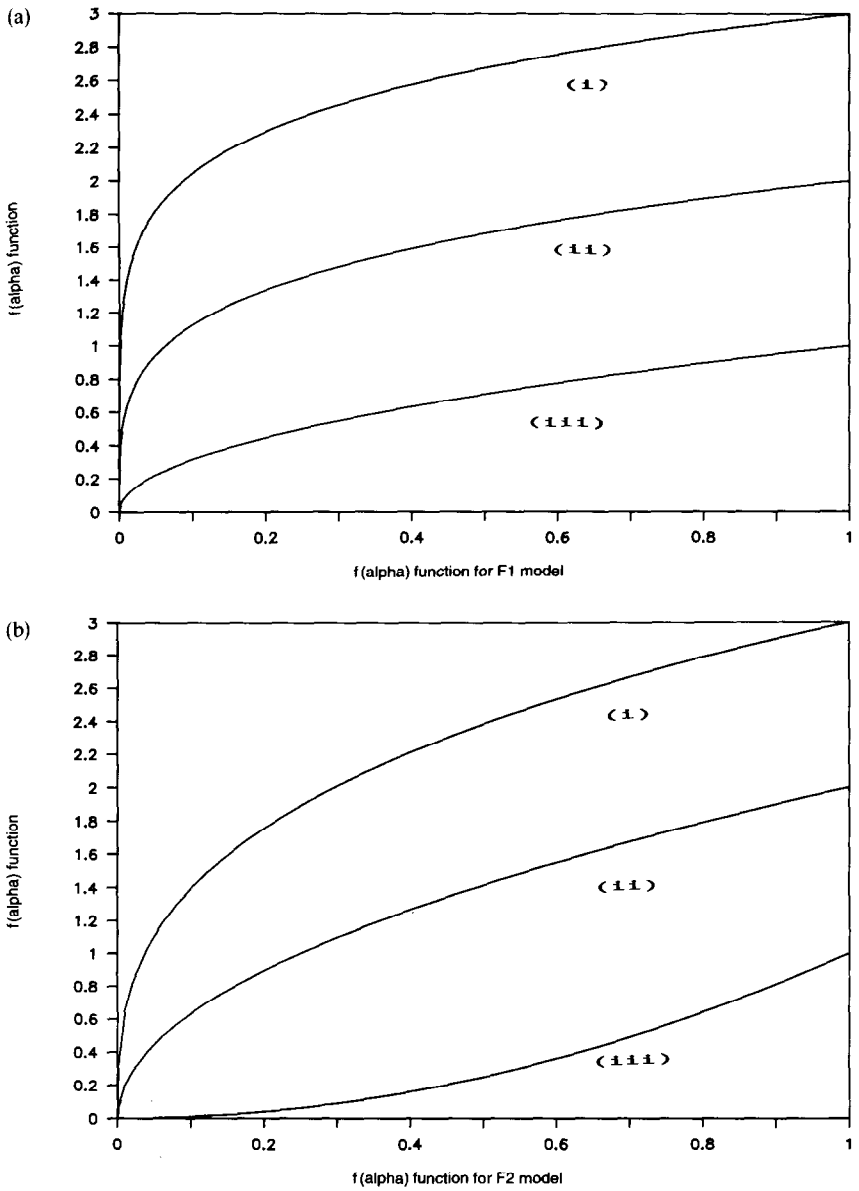

Fig. 4. Rate–rate plots:
(a) (i) $f(\alpha)$ function of R3 model against $f(\alpha)$ functon of F1 model;
(ii) $f(\alpha)$ function of R2 model against $f(\alpha)$ function of F1 model;
(iii) $f(\alpha)$ function of F2 model against $f(\alpha)$ function of F1 model.
(b) (i) $f(\alpha)$ function of R3 model against $f(\alpha)$ function of F2 model;
(ii) $f(\alpha)$ function of R2 model against $f(\alpha)$ function of F2 model;
(iii) $f(\alpha)$ function of F1 model against $f(\alpha)$ function of F2 model.
(c) (i) $f(\alpha)$ function of R3 model against $f(\alpha)$ function of R2 model;
(ii) $f(\alpha)$ function of F2 model against $f(\alpha)$ function of R2 model;
(iii) $f(\alpha)$ function of F1 model against $f(\alpha)$ function of R2 model.

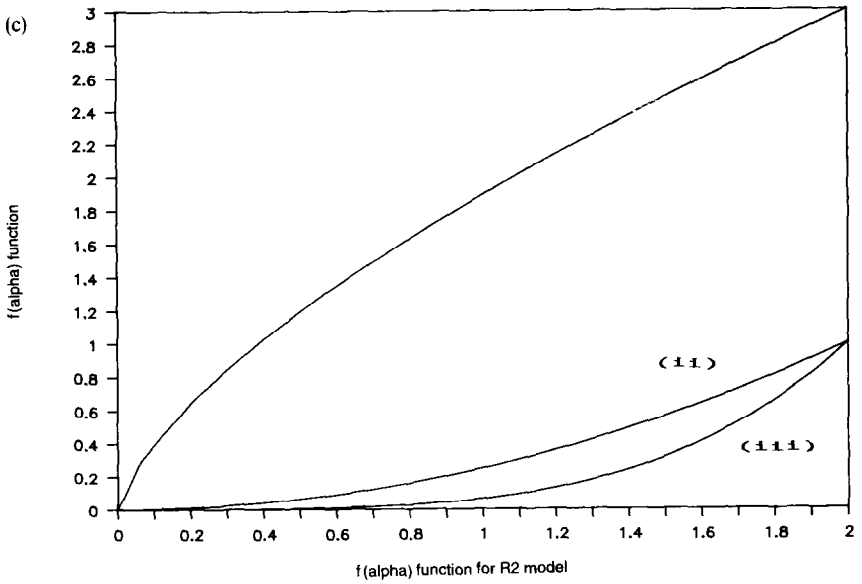

Fig. 4. (*Continued*)

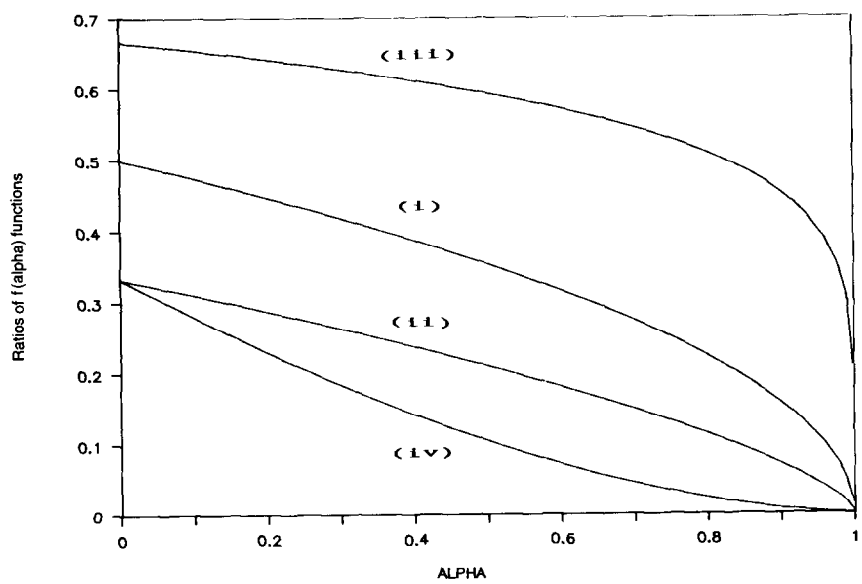

Fig. 5. Ratios of $g(\alpha)$ plots against α
(i) ($f(\alpha)$ function of F1 model/$f(\alpha)$ function of R2 model) against α;
(ii) ($f(\alpha)$ function of F1 model/$f(\alpha)$ function of R3 model) against α;
(iii) ($f(\alpha)$ function of R2 model/$f(\alpha)$ function of R3 model) against α;
(iv) ($f(\alpha)$ function of F2 model/$f(\alpha)$ function of R3 model) against α.

In the early stages of reaction, any rate equation based upon an expression of the form $f(\alpha) = v/k = N(1-\alpha)^n$, where N is a numerical constant, will not be very sensitive to the value of n, whether it is an integer or a fractional value. Plots of rate ($d\alpha/dt$) against α also enable the rate equation to be identified reliably. These rate equations are discussed further below in relation to their distinguishability from the following group of diffusion-based equations.

4.3. *Deceleratory diffusion and geometric kinetic models*

When this method of analysis is applied to the diffusion models D1, D2, D3 and D4 in the various binary combinations, the distinguishability is apparently extremely poor and all of the plots (not shown) appear to be linear. When individual points are plotted, it is seen that the majority of the points are clustered near the origin (high α and low rates). All of the $f(\alpha)$ expressions (Table 1) tend towards infinity at low values of α and to zero as α tends to 1.

Plots of the ratios of values of $f(\alpha)$ for pairs, selected from the D1, D2, D3 and D4 models, against α are shown in Fig. 6. Deviation from expected constancy is apparent, especially at high α, making this form of examination more effective.

In a further attempt to improve distinguishability, ln–ln plots were examined. The results are shown in Fig. 7. These plots give approximately parallel straight lines at low α values, with curvature developing towards the origin at (0,0). A useful indication of the correct choice of rate equation is that the ln–ln plot should be linear and pass through the origin. Distinguishability is best at high values of α in the region where the ln values become negative, and the curvature, and hence the value of the intercept on the y-axis when $x = 0$, is a guide to the direction in which kinetic analysis should continue. If the intercept is positive, models higher in the sequence D1, D2, D3, D4 should be tested, and if the intercept is negative, models earlier in the sequence are indicated.

In addition to distinguishing amongst the D1, D2, D3 and D4 models, it is necessary to examine the distinguishability of this group of models from the deceleratory geometric models (F1, R2, R3 and even second-order behaviour, F2). Since the ln–ln plots described above have shown promise, such plots were prepared for the F1, F2, R2 and R3 equations and are shown in Fig. 8. All of the plots shown are linear with different slopes, and points are clustered at low values of α. This is the opposite situation to that in the rate–rate plots for the diffusion models (Fig. 6).

Further ln–ln plots for the combinations of the four D1, D2, D3 and D4 rate equations in turn with each of the group F1, F2, R2 and R3 are shown in Fig. 9. All the plots are strongly curved and the linear plots obtained for the "correct" choices are shown for comparison.

As a further way of examining the constancy of the rate coefficient k_1 for the diffusion models, plots of the differences between $\ln f(\alpha)$ values for pairs of models against α are shown in Fig. 10. Such plots should in general give horizontal lines with ordinate equal to $\ln k_1$, and in these representations the ordinate is equal to zero since $k_1 = 1$.

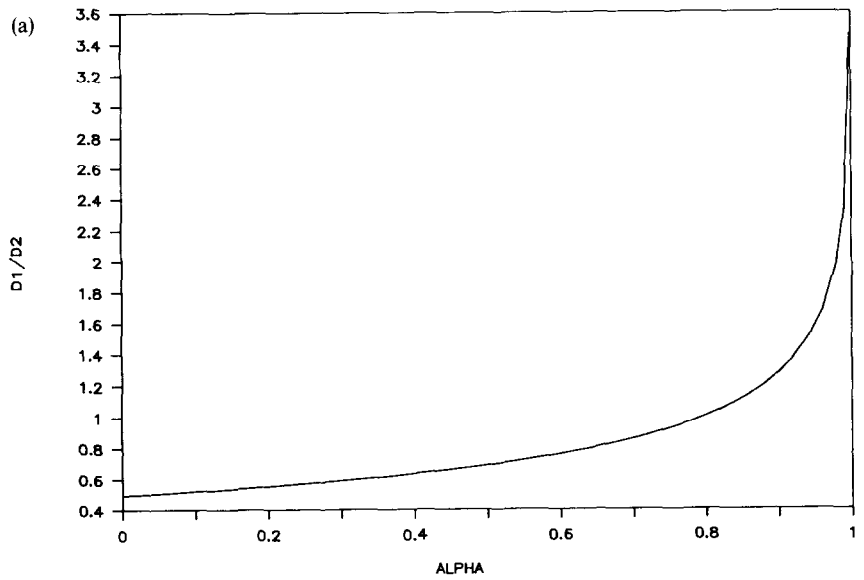

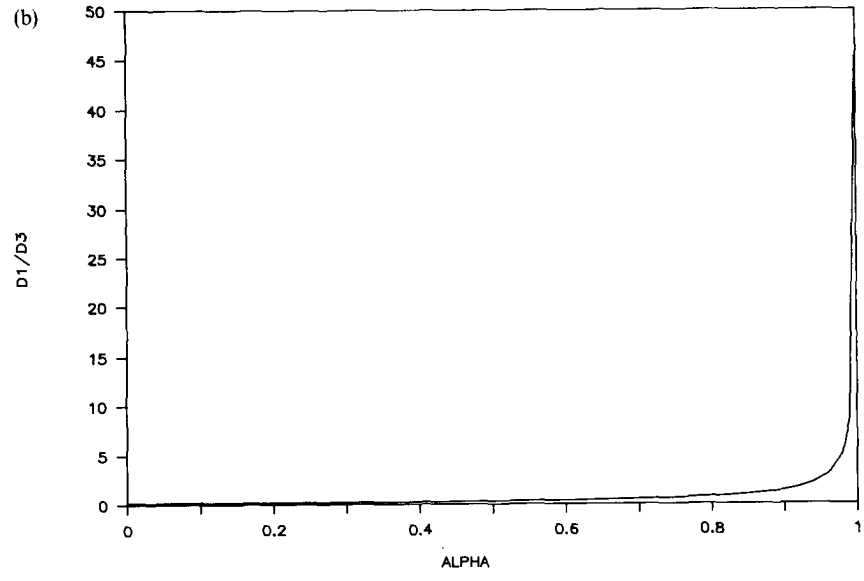

Fig. 6. (*Continued*)

(c)

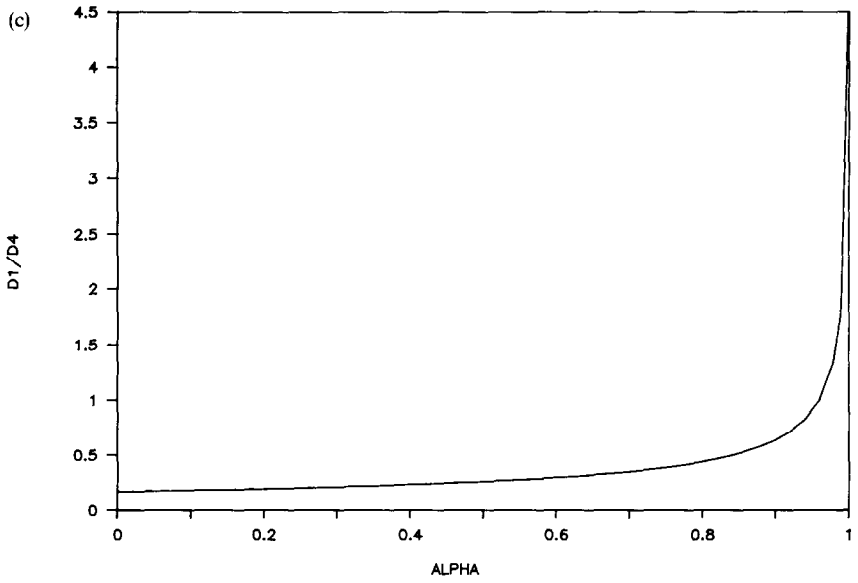

(d)

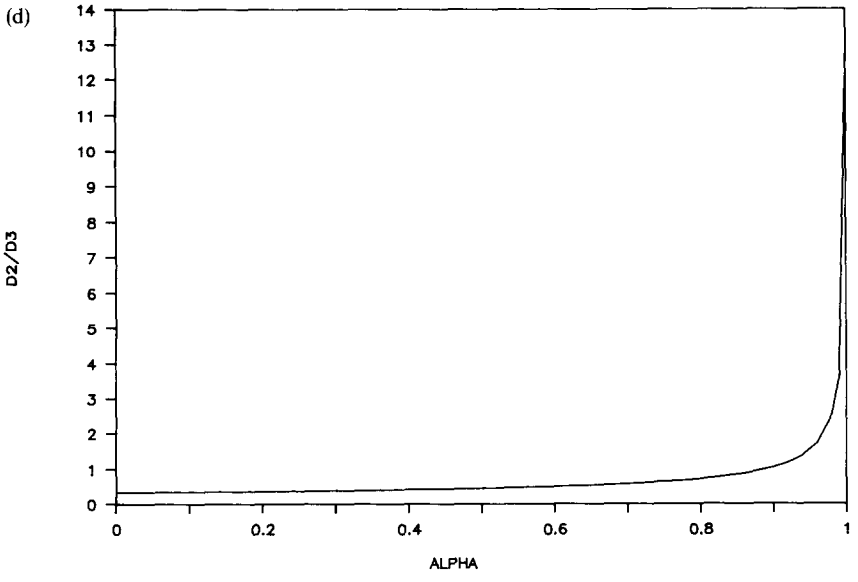

Fig. 6. (*Continued*)

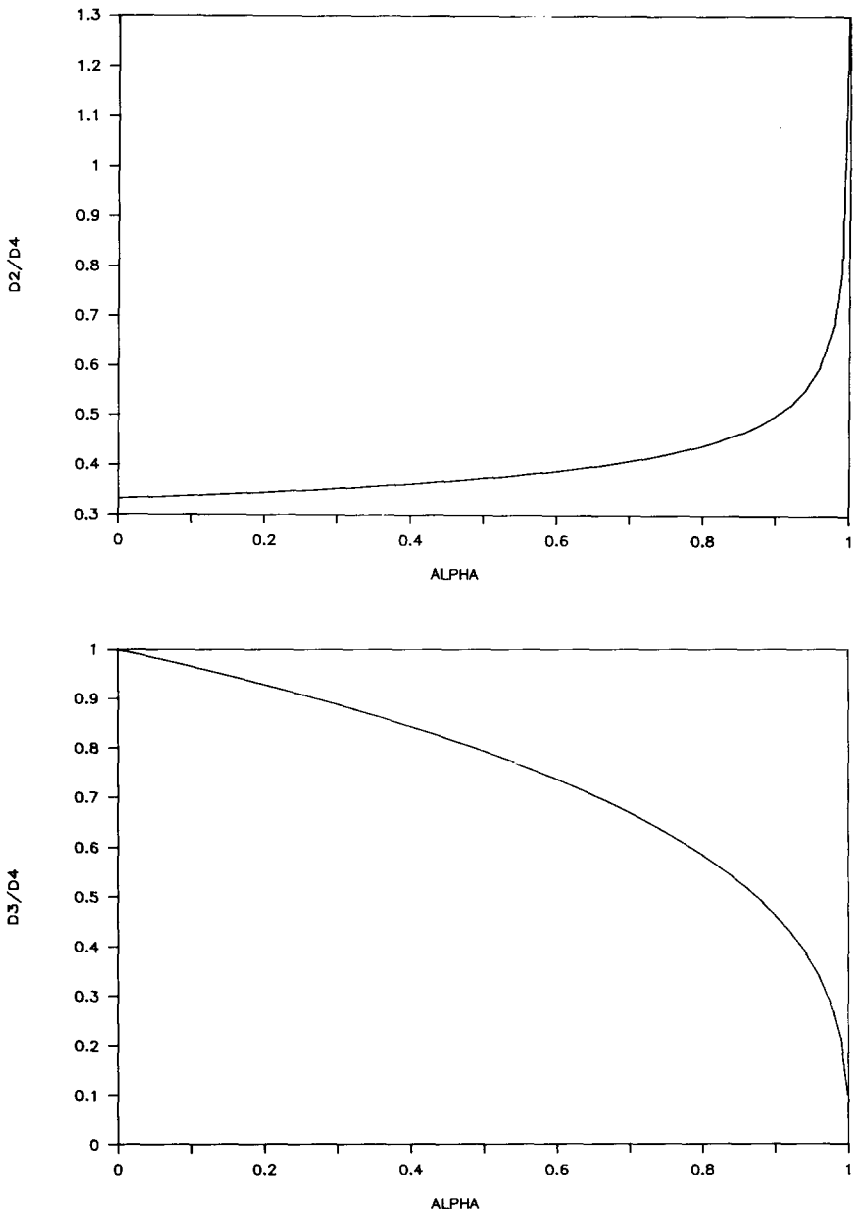

Fig. 6. Ratios of $f(\alpha)$ plots against α:
(a) ($f(\alpha)$ function of D1 model/$f(\alpha)$ function of D2 model) against α;
(b) ($f(\alpha)$ function of D1 model/$f(\alpha)$ function of D3 model) against α;
(c) ($f(\alpha)$ function of D1 model/$f(\alpha)$ function of D4 model) against α;
(d) ($f(\alpha)$ function of D2 model/$f(\alpha)$ function of D3 model) against α;
(e) ($f(\alpha)$ function of D2 model/$f(\alpha)$ function of D4 model) against α;
(f) ($f(\alpha)$ function of D3 model/$f(\alpha)$ function of D4 model) against α.

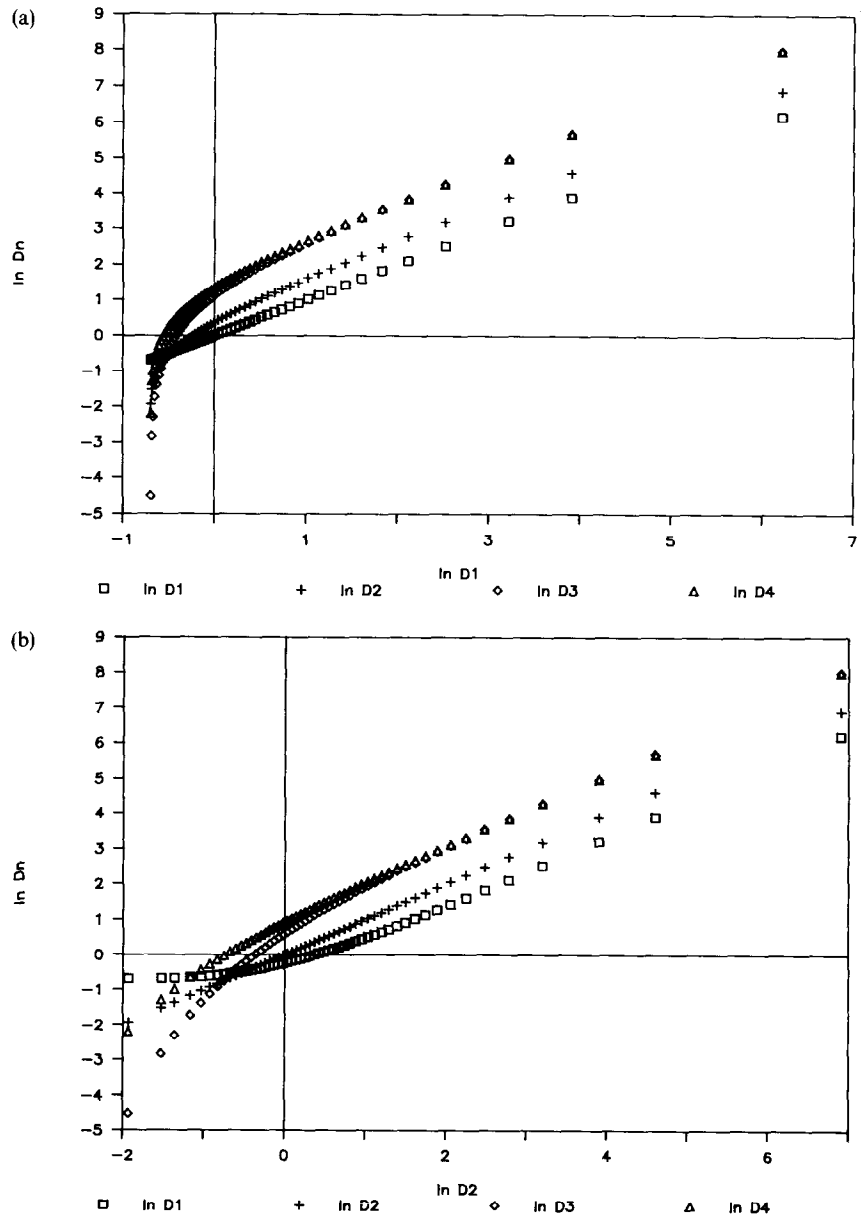

Fig. 7. Ln–ln plots.
(a) Ln($f(\alpha)$ function of Dn model) against ln($f(\alpha)$ function of D1 model): □, ln D1; +, ln D2; ◇, ln D3; △, ln D4.
(b) Ln($f(\alpha)$ function of Dn model) against ln($f(\alpha)$ function of D2 model): □, ln D1; +, ln D2; ◇, ln D3; △, ln D4.
(c) Ln(f(α) function of Dn model) against ln($f(\alpha)$ function of D3 model): □, ln D1; +, ln D2; ◇, ln D3; △, ln D4.
(d) Ln($f(\alpha)$ function of Dn model) against ln($f(\alpha)$ function of D4 model): □, ln D1; +, ln D2; ◇, ln D3; △, ln D4.

(c)

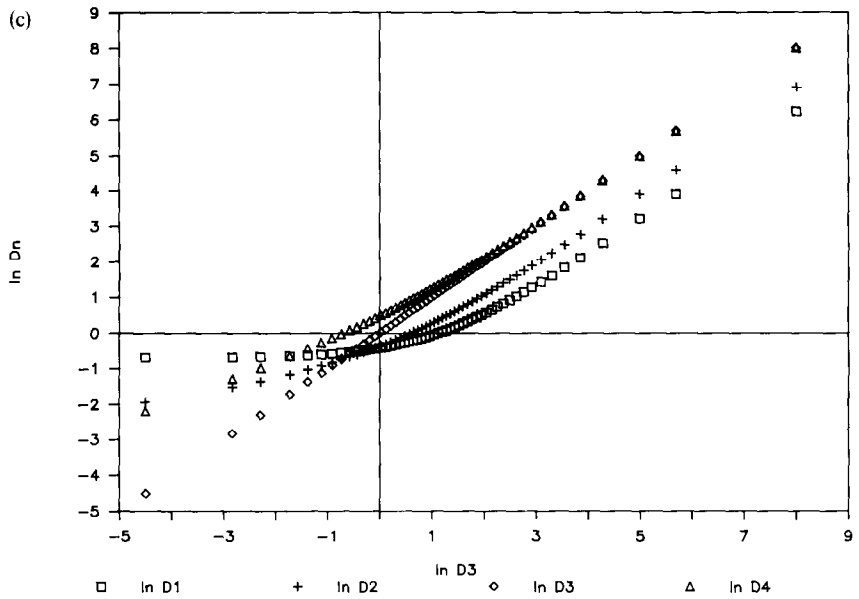

(d)

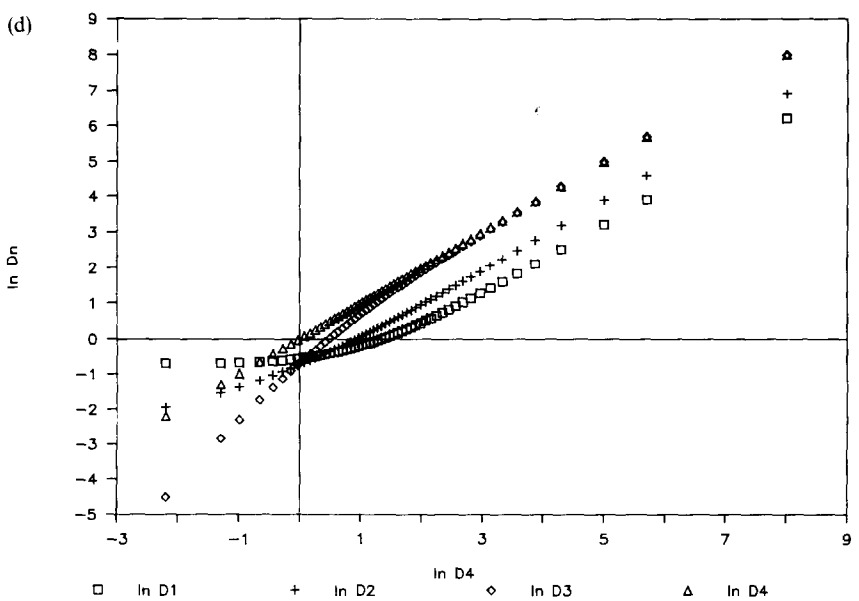

Fig. 7. (*Continued*)

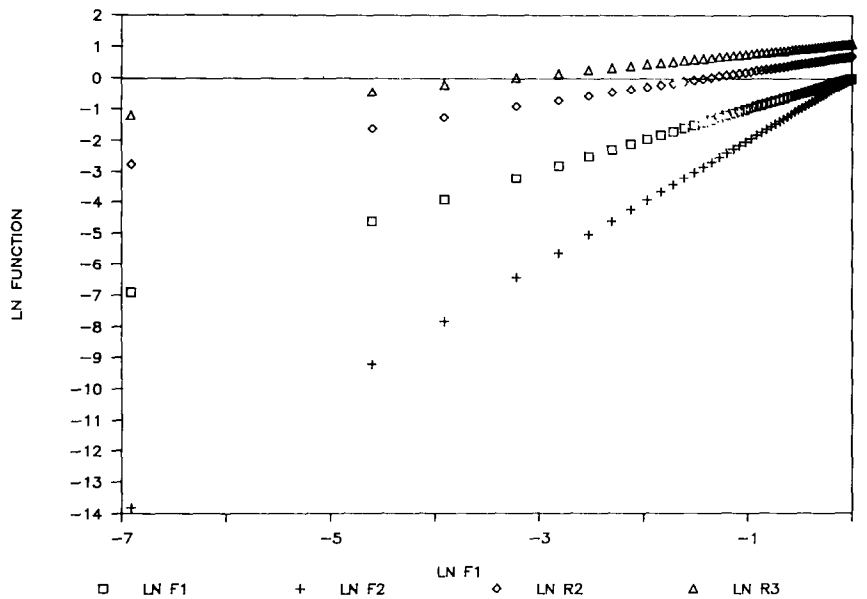

Fig. 8. Ln–ln plots. Ln($f(\alpha)$ functions of F1, F2, R2 and R3 models) against ln($f(\alpha)$ function of F1 model): □, ln F1; +, ln F2; △, ln R2; ◇, ln R3.

5. Discussion and conclusions

For a method which requires measurements of $d\alpha/dt$, α and t to have any advantage, the method would have to provide improved distinguishability amongst the model expressions. In common with other methods of kinetic analysis, the diffusion group of models presents problems. To improve distinguishability within this group, use may be made of ln–ln plots, i.e. plots of ln (experimental rate data) against ln($f(\alpha)$ values for the model being tested).

From the plots shown in Figs. 1–10, the following conclusions can be reached.

1. Plots of rate against $f(\alpha)$ will be linear if:
   (a) the correct rate equation has been applied in the analysis of the experimental data, or
   (b) the "correct" rate equation is one of the group D1, D2, D3 or D4, and one of these rate equations has been applied in the analysis of the experimental data.
2. Plots of ln (rate) against ln($f(\alpha)$) will be linear if:
   (a) the correct rate equation from the group D1, D2, D3 or D4, has been applied in the analysis of the experimental data, or
   (b) the "correct" rate equation is one of the group F1, F2, R2 or R3 and one of these four rate equations has been used in the analysis.
3. Examinations of plots of ratios of [experimental rates/calculated $f(\alpha)$] (for a selected model) against α for constancy provide the most useful information in that they immediately identify the region of α where deviation is greatest.

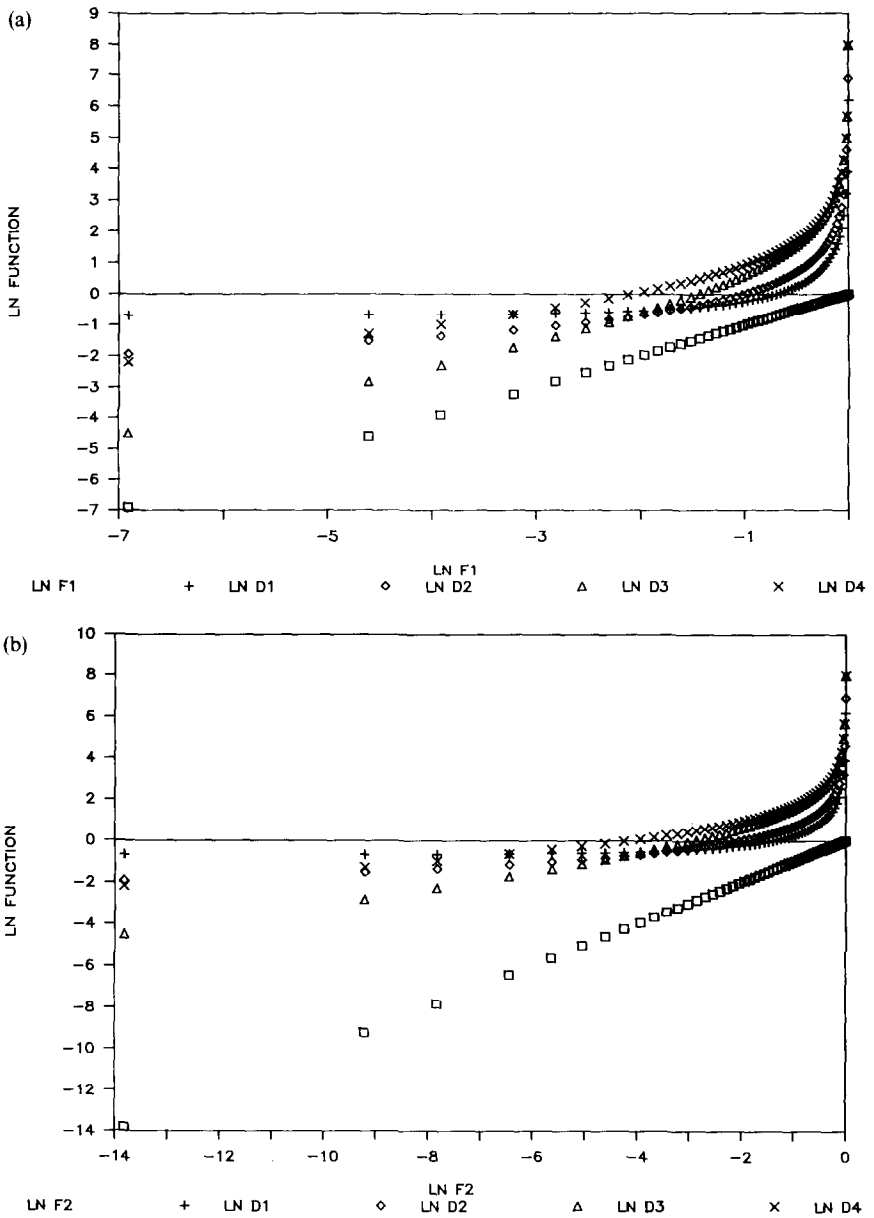

Fig. 9. Ln–ln plots.

(a) Ln($f(\alpha)$ function of Dn model) aganist ln($f(\alpha)$ function of F1 model): □, ln D1; +, ln D2; ◇, ln D3; △, ln D4.

(b) Ln($f(\alpha)$ function of Dn model) against ln($f(\alpha)$ function of F2 model): □, ln D1; +, ln D2; ◇, ln D3; △, ln D4.

(c) Ln ($f(\alpha)$ function of Dn model) against ln($f(\alpha)$ function of R2 model): □, ln D1; +, ln D2; ◇, ln D3; △, ln D4.

(d) Ln($f(\alpha)$ function of Dn model) against ln($f(\alpha)$ function of R3 model): □, ln D1; +, ln D2; ◇, ln D3; △, ln D4.

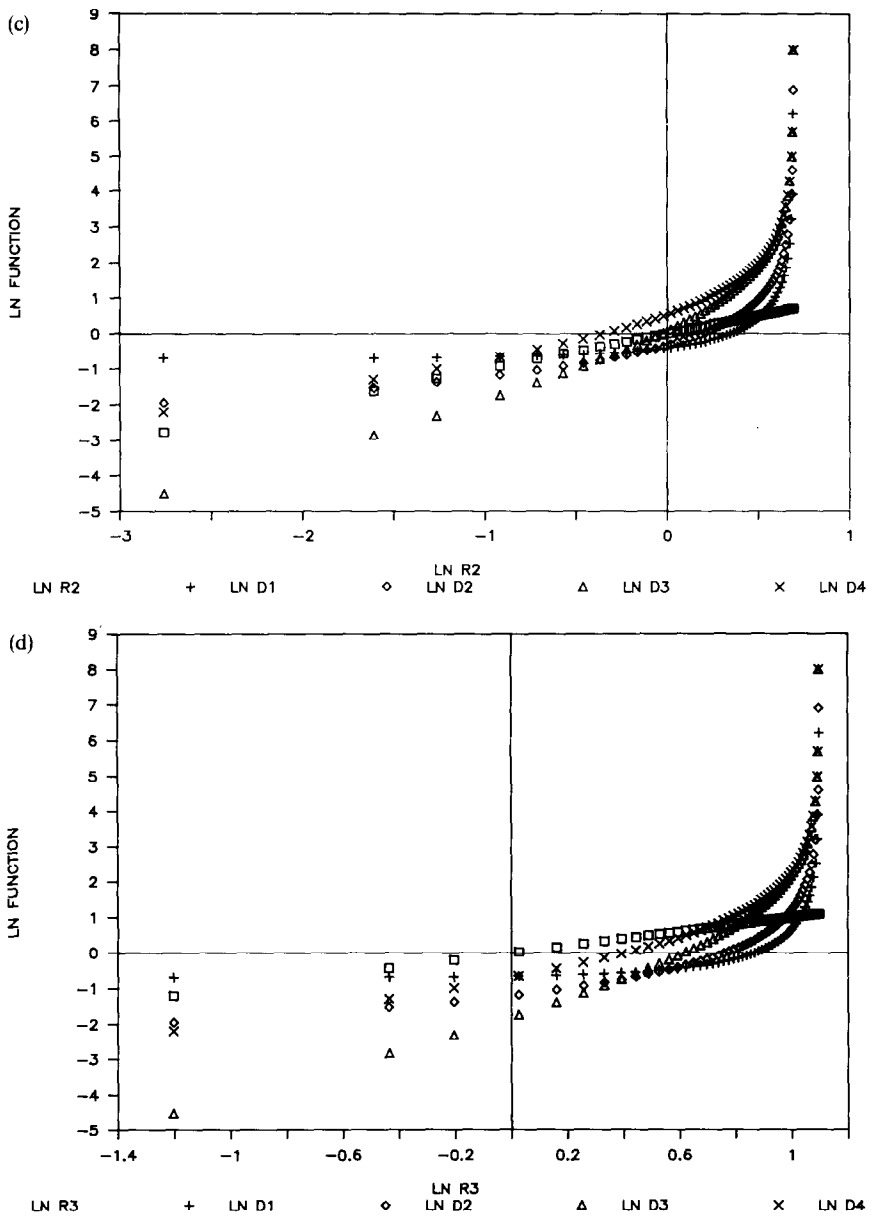

Fig. 9. (*Continued*)

4. From the scatter and deviations of the experimentally measured data on these graphs the accuracy and reliability of the values of the rate coefficients can be estimated. Where appropriate, this uncertainty can be included in the calculation of the activation energy.

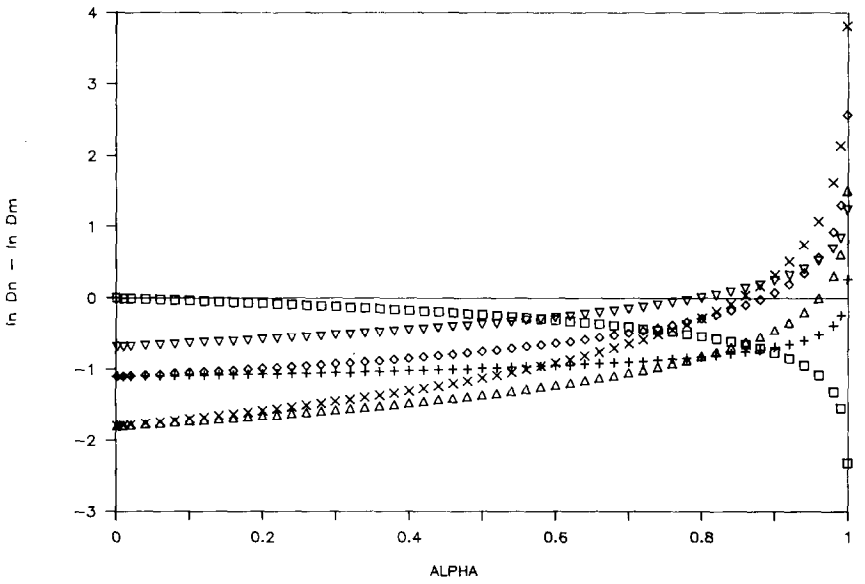

Fig. 10. Ln (rate) – ln($f(\alpha)$) plots against α:
▽, ln($f(\alpha)$ function of D1 model) – ln($f(\alpha)$ function of D2 model) against α;
×, ln($f(\alpha)$ function of D1 model) – ln($f(\alpha)$ function of D3 model) against α;
△, ln($f(\alpha)$ function of D1 model) – ln($f(\alpha)$ function of D4 model) against α;
◇, ln($f(\alpha)$ function of D2 model) + ln($f(\alpha)$ function of D3 model) against α;
+, ln($f(\alpha)$ function of D2 model) – ln(f/α) fnction of D4 model) against α;
□, ln($f(\alpha)$ function of D3 model – ln($f(\alpha)$ function of D4 model) against α.

This approach is also only of value where the kinetic data are of sufficient accuracy to enable differential measurements to be used. Distinguishability amongst the models considered here in the sigmoid group is good and is promising in the deceleratory geometrical group.

An experimental technique which provides a derivative output which can usually be directly related to $d\alpha/dt$ via the enthalpy of reaction, is isothermal DSC [20]. Such derivative measurements do, however, have to be distinguishable from the baseline (usually stable) and hence the method is not suitable for very slow processes. Self-heating or self-cooling of reactant crystallites may also impose restrictions on the highest reaction rates that may be measured. The difficulties with slow processes do not apply to isothermal DTG. The DSC signal may be masked to some extent by the characteristic instrument responses to changes from rapid heating to isothermal conditions. It is possible to eliminate the instrument responses by repeating the heating procedure on the "dead" sample and subtracting this record from that for the kinetic measurements.

Advances in the accuracy of rate measurements require improved methods of kinetic analysis. Comparisons of rates of reaction, rather than yield–time data, with theoretical expectation provide a method of improved discrimination. The present analysis

identifies the patterns of deviation arising from an incorrect selection of rate expression which may be useful in identifying the equation most closely describing the rate process being investigated. The conclusions of kinetic analysis must, as always, be supported by other experimental observations, notably microscopy.

References

[1] W.E. Garner (Ed.), Chemistry of the Solid State, Butterworth, London, 1955.
[2] D.A. Young, Decomposition of Solids, Pergamon, Oxford, 1966.
[3] B. Delmon, Introduction à la Cinétique Hétérogène, Technip, Paris, 1969.
[4] M.E. Brown, D. Dollimore and A.K. Galwey, Comprehensive Chemical Kinetics, Vol. 22, Elsevier, Amsterdam, 1980.
[5] J. Sestak, Comprehensive Analytical Chemistry, Vol. 12, Part D, Elsevier, Amsterdam, 1984.
[6] M.E. Brown and A.K. Galwey, Thermochim. Acta, 29 (1979) 129.
[7] N.J. Carr and A.K. Galwey, Thermochim. Acta, 79 (1984) 323.
[8] A.K. Galwey and G.M. Laverty, Solid State Ionics, 38 (1990) 155.
[9] A.K. Galwey, Thermochim. Acta, 96 (1985) 259; React. Solids, 8 (1990) 211.
[10] A.K. Galwey, J. Therm. Anal., 41 (1994) 267.
[11] M.E. Brown, A.K. Galwey and A. Li Wan Po, Thermochim. Acta, 203 (1992) 221; 220 (1994) 131.
[12] V.B. Okhotnikov, N.A. Baranov, G.M. Laverty and A.K. Galwey, Phil. Trans. R. Soc. (London), A347 (1994) 139, 157.
[13] S. Rajam and A.K. Galwey, J. Chem. Soc., Faraday Trans. 1, 78 (1982) 2553.
[14] A.K. Galwey and G.G.T. Guarini, Proc. R. Soc. London Ser. A, 441 (1993) 313.
[15] H. Tanaka and N. Koga, J. Am. Ceram. Soc., 49 (1966) 379.
[16] J.H. Sharp, G.W. Brindley and B.N.N. Achar, J. Am. Ceram. Soc., 49 (1966) 379.
[17] M.E. Brown, D. Dollimore and A.K. Galwey, J. Chem. Soc., Faraday Trans. 1, 70 (1974) 316; Thermochim. Acta, 21 (1977) 103.
[18] M. Selvaratnam and P.D. Garn, J. Am. Chem. Soc., 59 (1976) 376.
[19] M.E. Brown and A.K. Galwey, Anal. Chem., 61 (1989) 1136.
[20] M.E. Brown and A.K. Galwey, Thermal Analysis, Proc 7th ICTA, Wiley-Heyden, Chichester, 1 (1982) 58.
[21] W.-L. Ng, Aust. J. Chem., 28 (1975) 1169.
[22] D.N. Waters and J.L. Paddy, Anal. Chem., 60 (1988) 53.
[23] F. Mata-Perez and J.F. Perez-Benito, J. Chem. Educ., 64 (1987) 925.
[24] A.K. Galwey, J. Chem. Soc. A (1966) 87.